LIMOLIT – A NOVEL THERMOGRAPHIC CHARACTERISATION METHOD FOR P/N STRUCTURES AND SOLAR CELLS

M. Kaes, S. Seren, T. Pernau, G. Hahn

University of Konstanz, Department of Physics, PO Box X916, 78457 Konstanz, Germany

Tel: +49-7531-88-2082, Fax: +49-7531-88-3895. Email: martin.kaes@uni-konstanz.de

ABSTRACT: In this contribution a new thermographic measurement technique is presented which allows the detection of shunts and recombination in p/n-structures as well as metallized solar cells. The method uses the well established lock-in thermography principle, but the necessary reference is applied by modulated light. The device subject to illuminated thermography measurements can be operated at mpp conditions in all aspects, esp. carrier density and transport. Defects are visualized according to their true impact on solar cell performance. The comparison with classical lock-in thermography shows that the new method is also sensitive to thermalisation losses of photogenerated carriers. Illuminated thermography measurements can reveal defects that are not detectable with the conventional method, e.g. current losses through npn or pnp structures. A monitoring of shunt generation is possible by measurements before and after problematic processing steps, e.g. metallization. As the light modulated lock-in thermography technique is fast and contactless, it is suitable for inline process monitoring and industry.

Keywords: Characterisation - 1, Shunts - 2, Defects - 3

1 INTRODUCTION

Thermographic investigations of solar cells using an infrared (IR) sensitive camera can be used to detect weak current leaks (shunts) at defects and impurities or process induced damages due to their local heat generation [1,2]. To raise the signal-to-noise ratio, Lock-In Thermography (LIT) [3,4] based on an externally modulated voltage applied via the metal contacts of the solar cell is applied. However, with LIT, a metallization of the solar cell is coercible required. As this is one of the last steps in the fabrication process of solar cells, thermographic analysis of shunts was so far restricted to processed solar cells. This restriction can be overcome with the new Light-modulated Lock-In Thermography technique (LimoLIT).

2 LOCK-IN THERMOGRAPHY

2.1 Experimental setup
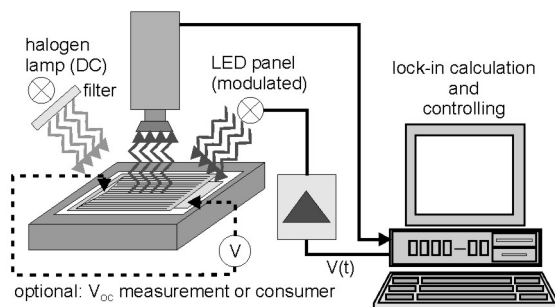
Figure 1: Experimental setup of the LimoLIT measurement assembly [5,6]. The modulated Lock-In reference signal is applied by an array of LEDs (pulsed light). A halogen lamp can provide constant bias light. No contacting is required, a wafer with p/n junction is sufficient.

For conventional Voltage-modulated Lock-In Thermography (in the following refered as VomoLIT) the reference signal is generated by an AD/DA interface card and subsequently amplified. This signal is applied to the solar cell by a probe via the front finger grid and the backside metallization. The solar cell is fixed on a temperature stabilized chuck. The IR camera (3-5 μm range by Cedip, distributed by InfraTec) delivers at discrete adjustable time intervals temperature images of the solar cell with a noise level of σ_C=20 mK for each pixel. The subsequent lock-in calculation is performed by the computer in real-time with a self-developed software.

The lateral resolution of the shunts is enhanced by the use of the modulation due to the exponential decay of periodically generated heat waves [3] as compared to the steady-state operation. The lock-in calculation provides not only the signal magnitude but also the phase delay which contains additional information [7,8,12]. The lock-in calculated magnitude for a camera system with a frame rate f_C and camera noise σ_C after a measurement time t has a noise level of

$$\sigma = \frac{2\sigma_C}{\sqrt{f_C \cdot t}} . \qquad (1)$$

This leads to a fast noise reduction within the first few seconds of measurement.

For LimoLIT measurements a LED array illuminates the wafer containing a p/n junction or the solar cell. The modulated flow of charge carriers is generated by the device itself, contacts are not required. Therefore, solar cells can be measured already in early stages of processing, enabling a thermographic process monitoring. Potential shunts can be spotted after individual fabrication steps of solar cells without any risk of a possible contamination. An optional electric contacting can be used to measure the light-generated voltage of metallized solar cells and to adjust the incident light intensity.

2.2 LimoLIT - theoretical consideration

The signal generating effects relevant for LimoLIT are demonstrated in the band model shown in Fig. 2. The model describes an illuminated p/n structure with a (local) shunt resistance connected parallel to the (widespread) diode. Most of the light generated electron/hole pairs are separated by the p/n junction, so that the movement of these carriers is mainly governed by the conductivity of the emitter. A local shunt resistor draws a photocurrent from the p/n structure. The area contributing to this photocurrent is limited by the conductivity of the emitter and the incident photon flux.

In case of a metallized solar cell, the metallization can effectively collect the photocurrent of the whole device and therefore increase carrier transport to the shunt. The energy deposited by each carrier is expected to be $q \cdot V_{oc}$, with V_{oc} the open circuit voltage reached by the shunted device and the elementary charge q.
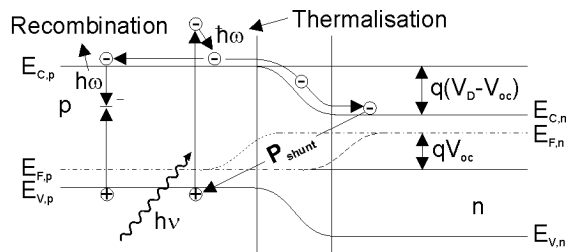

Figure 2: The electron/hole pair generated by light absorption carries excess photon energy. A charge carrier separated by the p/n junction gains the potential energy $q \cdot (V_D - V_{oc})$. Thus, the total energy deposited at a shunt close to carrier separation is higher than $q \cdot V_{oc}$.

In case of LimoLIT, one has to take into account the origin of the carriers consumed by the shunt due to a generation over the entire cell area and not only due to a injection via the finger grid covering only a small part of the cell area (VomoLIT). Regarding a shunt located underneath a grid finger, an externally (VomoLIT) or internally (LimoLIT) in the metallisation injected carrier transports the energy of $q \cdot V_{oc}$. Solely in LimoLIT a fraction of the current flows laterally from the position of generation through the emitter. This enhances the transported energy per charge carrier due to the carriers affiliation to the conduction band respectively the valence band. Therefore it's energy is higher than $q \cdot V_{oc}$. From these considerations we expect the LimoLIT signal to be stronger than the VomoLIT signal under comparable V_{oc} conditions.

3 RELATION BETWEEN LIMOLIT AND VOMOLIT

3.1 Thermalisation in LimoLIT
LimoLIT mainly differs from VomoLIT by a homogeneous signal offset distributed over the whole illuminated area. This is the consequence of a heat generation by the incident photon flux not converted into electrical energy. One part of this effect is the thermalisation by a rather fast decay of the excess photon energy after indirect absorption in silicon. This warming depends strongly on the photon wavelength. Whereas for yellow light (551 nm) the thermalisation energy is half of the photon energy, this effect becomes almost negligibly for infrared illumination in the range of the band gap. Another heat generating process is non-radiative recombination. The additional signal introduced by these effects can either be reduced by using longer irradiation wavelengths as long as recombination remains dispensable, or by decreasing the applied light intensity. The latter is a compromise as this results in a lower induced voltage which decreases signal strength and therefore leads to a longer measurement time. Fig. 3 shows the effect of thermalisation for two different wavelengths of the incident light.
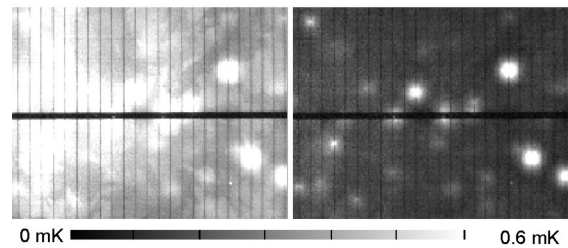
Figure 3: Comparable LimoLIT measurements of a solar cell performed under cyan illumation (505 nm, left) and IR illumination (880 nm, right). The corresponding generated open circuit voltage is 365 mV for both measurements. The inhomogeneities visible in the left part of the left measurement are due to a non-uniform illumination.

3.2 Comparison of both techniques
To compare the two techniques under similar conditions, measurements on a metallized solar cell were carried out. The voltage modulation in LimoLIT generated by modulated and additional constant bias light was measured and adjusted to the same value as applied for the VomoLIT method. Other parameters like measurement time, camera settings and lock-in frequency have been identical, too.
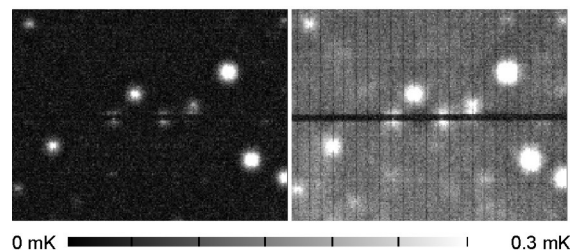
Figure 4: Left: VomoLIT, right: LimoLIT measurement. The rectangular voltage modulation results in 0-320 mV for both techniques.

Both measurements shown in Fig. 4 are qualitatively equivalent apart from the background signal visible in the LimoLIT mapping. Quantitatively, LimoLIT shows stronger power losses at shunt positions. The voltage modulation induced either by the illumination or the applied bias voltage is 320 mV for both measurements. Ohmic shunts are dominating the power losses in this voltage range and a similar behavior
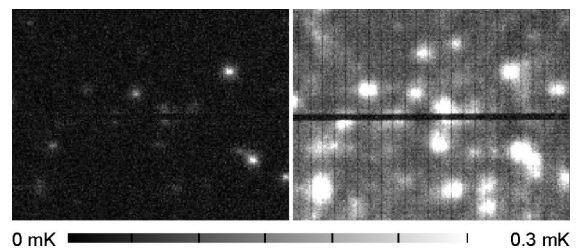
Figure 5: Same setup as presented in Fig. 4, now with additional constant bias. LimoLIT (right) now shows a multitude of shunts, which cannot be identified in VomoLIT. The constant bias corresponds to 400 mV DC voltage, the modulation was adjusted to 50 mV. The intensity of the modulated light is the same as in Fig. 4.

is therefore expected for both methods. This changes if an additional constant bias is applied as illustrated in Fig. 5. The nature of the shunts is responsible for the general difference between Fig: 4 and 5. Whereas the influence of ohmic shunts decreases because of the smaller voltage modulation as compared to Fig. 4, power losses due to Schottky-type shunts become more important because of their increasing electrical conductivity in this voltage range [6].

3.3 Realistic measurement conditions with LimoLIT

The current flow for the LimoLIT technique is the same as for the illuminated solar cell under operation. Therefore, LimoLIT measurements under a constant bias light simulating V_{oc} or working point conditions if an external consumer is attached enable the visualization of relevant shunts affecting the solar cell parameters. In conventional VomoLIT the current flow across the p/n junction is in opposite direction and the lateral flow through the emitter is neglected, as the current is injected only via the front finger grid metallisation.

4   NEW APPLICATIONS FOR LIMOLIT

4.1 Detection of unwanted emitters

Besides the metallized emitter at the front side of standard industrial solar cells it is possible that there are additional emitter regions in the device. These can be inversion areas due to precipitates or emitter residues depending on the process sequence applied. One common issue is a $POCl_3$ emitter at the edge of the cell's backside. This occurs if the BSF after screen printing and firing does not cover the entire back surface of the solar cell. A previously diffused double-sided emitter is not overcompensated there. Like the front side emitter, this emitter collects carriers from the base. The rear side emitter residue will leak its photocurrent to the shunt across the rear side p/n junction. This reduces the photocurrent without changing the shape of the IV-curve of the solar cell. As the rear side emitter residue does not have a direct electrical connection to the front side, this effect can be made visible by an illuminated measurement only.
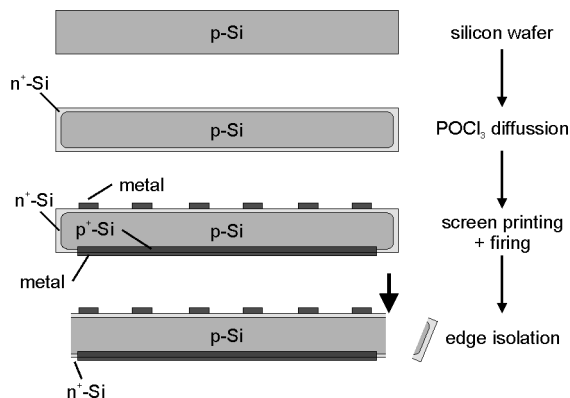

Figure 6: If the back side BSF does not cover the entire surface, a previously diffused emitter remains on the backside of the solar cell. This emitter residue may create rear side shunts.
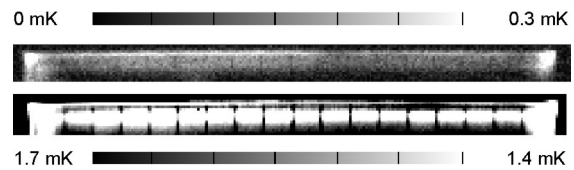
Figure 7: VomoLIT (top) and LimoLIT (bottom) measurement of a screen printed solar cell (Cz silicon). In contrast to VomoLIT, LimoLIT shows a strong signal at the interface of the rear side emitter and the BSF.

4.2 Shunt monitoring

LimoLIT measurements can be performed as soon as a carrier separating p/n-junction is defined. This creates the possibility to examine individual solar cell process steps by LimoLIT for shunt monitoring. An example for a shunt monitoring in an industrial solar cell process is shown in Fig. 8.
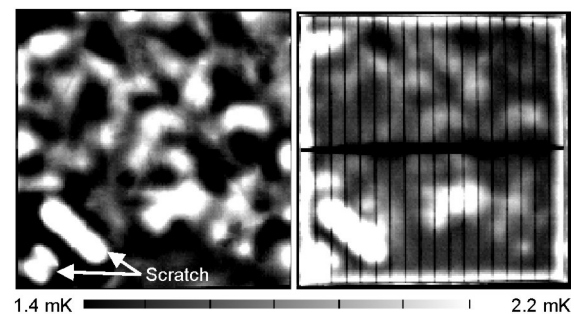

Figure 8: LimoLIT measurements performed after $POCl_3$ diffusion of a 5x5 cm² mc wafer (left) and of the processed solar cell (right, fill factor 75%). The emitter was intentionally scratched after $POCl_3$ diffusion. Already after emitter diffusion various heat sources are visible. In the end they are responsible for a reduced cell efficiency.

A solar cell was processed from a mc-silicon wafer using a standard firing-through SiN process with screen printed contacts [9]. After $POCl_3$ emitter diffusion the wafer was measured by the LimoLIT method using infrared LEDs (880 nm) without applying an additional constant bias light. The measurement reveals several weak heat sources. The emitter was intentionally scratched to simulate a process induced damage of the wafer (see arrows). The comparison of a high resolution LimoLIT measurement with an IQE mapping at 980 nm (Fig. 9) shows a good correlation of heat signals with areas of low IQE. This supports the assumption that recombination effects are visible in LimoLIT measurements already after emitter diffusion.

4.3 Fast measurements

The typical lock-in behaviour according to equation (1) gives an efficient noise reduction within a few seconds. Longer measurements show reduced background noise levels, whereas large signal components remain nearly unchanged. This effect is demonstrated in Fig. 10 by a comparison of a high-quality (2 h) and a fast (2 s) measurement.
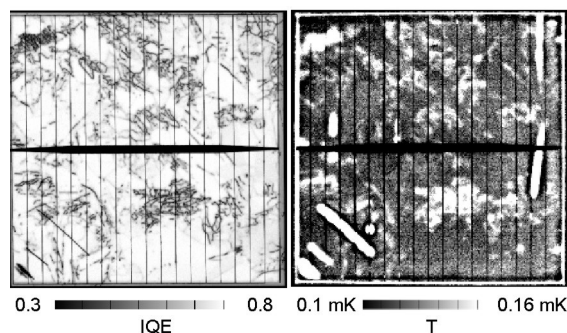
Figure 9: The comparison of a LBIC (left) and a LimoLIT (right) measurement shows a strong correlation between areas of low IQE and areas of multiple heat sources. Both effects can be related to areas of high recombination, e.g. grain boundaries.
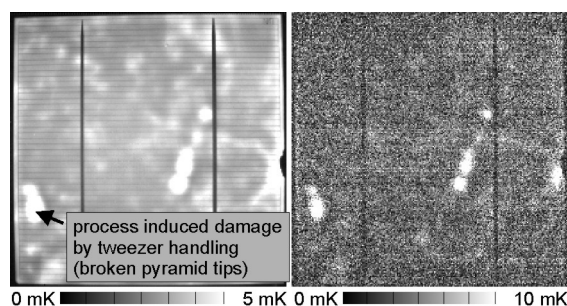
Figure 10: Comparison of a high quality measurement (2 h, left) and a fast measurement (2 s, right) of an acidic textured industrial-type solar cell with a fill factor of 75% (12.5x12.5 cm², screen printed). Even after only 2 s of measurement time process induced damages are revealed.

Most of the shunts visible in the high quality image can be detected already in the fast measurement. These rapidly detectable shunts are responsible for a reduced fill factor of 75% instead of an expected fill factor of 77%. The possibility to measure relevant shunts fast and contactless gives LimoLIT the potential to be applied for inline process control.

4.4 Current investigations

Complete process monitorings are currently performed using the LimoLIT technique. After each step of a solar cell process, typically starting with a POCl$_3$ emitter diffusion, the wafers are inspected for suspicious heat sources [10]. These defects as well as an inhomogeneous or locally missing emitter can generate shunts. The result indicates whether shunts are material induced or originating from the various subsequent process steps, e.g. screen printing. Therefore, a shunt-inducing process step can be identified and an optimization of the according step can be implemented subsequently.

Further on, different silicon materials can be investigated for intrinsic material defects in a convenient way. This can save a more complex analysis or a complete processing of a solar cell.

Shunts below grid lines are investigated for whether being ohmic or Schottky-type resistors [11].

5 SUMMARY

LimoLIT is able to determine current leaks in solar cells as well as VomoLIT does. As the voltage is generated by the sample internally the method is contactless. In contrast to VomoLIT this allows measurements on p/n structures without a metallization and enables a monitoring of emerging shunts during solar cell processing. LimoLIT approaches standard operating conditions of solar cells as close as possible.

6 ACKNOWLEDGEMENTS

7 REFERENCES

[1] A. Rogalski, K. Chrzanowski, Opto-electronics review 10(2) (2002) 111

[2] M. Dauner, K. Bücher, Proc. 26th IEEE PVSC, Anaheim 1997, 1137

[3] O. Breitenstein, M. Langenkamp, Lock-in Thermography, Basics and Use for Functional Diagnostics of Electronic Components, (Springer, Berlin, Heidelberg, New York, 2003)

[4] O. Breitenstein, M. Langenkamp, Proc. 2nd WC PVSEC, Vienna 1998, 1382

[5] M. Kaes, Master thesis, University of Konstanz (2003)

[6] M. Kaes, S. Seren, T. Pernau, G. Hahn, Prog. Photovolt: Res. Appl. 12 (2004) in press

[7] T. Pernau, P. Fath, E. Bucher, Proc. 29th IEEE PVSC, New Orleans 2002, 442

[8] X.P.V. Maldague, Theory and Practice of Infrared Technology for Nondestructive Testing (Wiley: New York, 2001)

[9] G. Hahn, S. Seren, D. Sontag, A. Gutjahr, L. Laas, A. Schönecker, Proc. 3rd WC PVSEC, Osaka 2003, 1285

[10] J. Arumughan, T. Pernau, this conference

[11] F. Huster, S. Seren, G. Schubert, M. Kaes, G. Hahn, O. Breitenstein, this conference

[12] Thomas Pernau, Impulse für die industrielle Produktion kristalliner Siliziumsolarzellen, PhD thesis, University of Konstanz, 2003